

# $\mu$ -hybrid inflation, gravitino dark matter, and stochastic gravitational wave background from cosmic strings

Adeela Afzal<sup>1</sup>,<sup>✉</sup> Waqas Ahmed,<sup>2</sup> Mansoor Ur Rehman<sup>1,\*</sup> and Qaisar Shafi<sup>3</sup>

<sup>1</sup>*Department of Physics, Quaid-i-Azam University, Islamabad, 45320, Pakistan*

<sup>2</sup>*School of Mathematics and Physics, Hubei Polytechnic University, Huangshi 435003, China*

<sup>3</sup>*Bartol Research Institute, Department of Physics and Astronomy, University of Delaware, Newark, Delaware 19716, USA*



(Received 16 February 2022; accepted 18 May 2022; published 31 May 2022)

We present a successful realization of supersymmetric  $\mu$ -hybrid inflation model based on a gauged  $U(1)_{B-L}$  extension of the minimal supersymmetric standard model, with the soft supersymmetry breaking terms are playing an important role. Successful nonthermal leptogenesis with gravitino dark matter yields a reheat temperature in the range  $2 \times 10^7 \lesssim T_R \lesssim 5 \times 10^9$  GeV. This corresponds to the predictions  $2 \times 10^{-18} \lesssim r \lesssim 4 \times 10^{-13}$  for the tensor to scalar ratio, and  $-2 \times 10^{-6} \lesssim dn_s/d \ln k \lesssim -5 \times 10^{-11}$  for the running of the scalar spectral index. The  $B-L$  breaking scale is estimated as  $6 \times 10^{14} \lesssim M/\text{GeV} \lesssim 10^{16}$ , calculated at the central value of the scalar spectral index,  $n_s = 0.9655$ , reported by Planck 2018. Finally, in a grand unified theory setup the dimensionless string tension parameter associated with the metastable strings is in the range  $10^{-9} \lesssim G\mu_{cs} \lesssim 10^{-6}$  corresponding to a stochastic gravitational wave background lying within the  $2\sigma$  bound of the recent NANOGrav 12.5-yr data.

DOI: [10.1103/PhysRevD.105.103539](https://doi.org/10.1103/PhysRevD.105.103539)

## I. INTRODUCTION

Supersymmetric (SUSY) hybrid inflation [1–8] offers an attractive framework for linking inflation with particle physics models based on grand unified theories (GUTs) [6]. In the minimal models [7,8], the soft supersymmetry breaking terms play an important role in making the predictions for the scalar spectral index  $n_s$  consistent with the cosmic microwave background (CMB) data [9,10]. Alternatively, the nonminimal terms in the Kähler potential serve a similar purpose [11–15]. With regard to linking inflation with particle physics models,  $\mu$ -hybrid inflation [16,17] offers an interesting class of SUSY hybrid inflation models where the  $\mu$ -problem of the minimal supersymmetric standard model (MSSM) is also resolved [16,18]. It is shown in [17] that  $\mu$ -hybrid inflation based on a renormalizable superpotential and minimal (canonical) Kähler potential leads to split supersymmetry scale with the gravitino mass,  $m_{3/2} \lesssim 5 \times 10^7$  GeV. However, with nonminimal Kähler potential we can realize  $\mu$ -hybrid inflation with  $m_{3/2} \sim 1$ –100 TeV and reheat temperature  $T_R \gtrsim 10^6$  GeV [19]. A shifted version of  $\mu$ -hybrid inflation

is investigated in [20] where the monopole problem associated with the breaking of the underlying gauge symmetry can be avoided. A viable model for gravitino dark matter and potentially detectable primordial gravitational waves are among the attractive features of these models. A discussion of successful leptogenesis in  $\mu$ -hybrid inflation, however, is missing in these papers which is one of the motivations of this paper.

A minimal version of  $\mu$ -hybrid inflation is considered in the present paper with renormalizable superpotential and minimal (canonical) Kähler potential. As compared to an earlier treatment of this model in [19], we here allow the soft SUSY breaking mass,  $M_S$ , to be different from the gravitino mass  $m_{3/2}$ , as assumed in [8] for standard SUSY hybrid inflation model. This leads to interesting consequences related to the viability of  $\mu$ -hybrid inflation with gravitino dark matter and successful nonthermal leptogenesis. An adequate range of reheat temperature is obtained while avoiding the gravitino overproduction problem [21,22].

This realization of  $\mu$ -hybrid inflation is based on a gauged  $U(1)_{B-L}$  extension of MSSM, where  $B$  and  $L$  are the baryon and lepton numbers respectively. The breaking of  $U(1)_{B-L}$  gives rise to a topologically stable cosmic string network that is usually constrained from the various experimental bounds. However, here we consider metastable cosmic strings where these bounds can be relaxed. A brief discussion related to the formation of such a metastable string network is presented in a GUT setup based on  $SO(10)$ .

\*mansoor@qu.edu.pk

Published by the American Physical Society under the terms of the [Creative Commons Attribution 4.0 International license](https://creativecommons.org/licenses/by/4.0/). Further distribution of this work must maintain attribution to the author(s) and the published article's title, journal citation, and DOI. Funded by SCOAP<sup>3</sup>.

This metastable cosmic string network can decay via the Schwinger production of monopole-antimonopole pairs [23] while generating a stochastic gravitational wave background (SGWB) in a range accessible at the ongoing and future gravitational wave (GW) experiments. We compare our model predictions with the recent bounds from the North American Nanohertz Observatory for Gravitational Waves (NANOGrav) 12.5-yr data [24]. In addition, we highlight the parameter space which is also consistent with gravitino dark matter and successful leptogenesis. For a similar study in no scale inflation see [25].

## II. SUPERSYMMETRIC $\mu$ -HYBRID INFLATION

The superpotential for hybrid inflation in a  $U(1)_{B-L}$  extension of minimal supersymmetric standard model (MSSM) can be written as [26–28],

$$W = \kappa S(\Phi\bar{\Phi} - M^2) + \lambda S H_u H_d + y_{ij}^{(U)} Q_i U_j^c H_u + y_{ij}^{(D)} Q_i D_j^c H_d + y_{ij}^{(L)} L_i E_j^c H_d + y_{ij}^{(\nu)} L_i H_u N_j^c + \frac{\lambda_{ij}}{M_*} \bar{\Phi}^2 N_i^c N_j^c, \quad (1)$$

where,  $i, j = 1, 2, 3$  are the family indices,  $\kappa, \lambda$  and  $\lambda_{ij}$  are dimensionless couplings and  $y_{ij}^{(U)}, y_{ij}^{(D)}, y_{ij}^{(L)}$  and  $y_{ij}^{(\nu)}$  are the Yukawa couplings, involving MSSM superfields,  $(Q_i, U_i^c, D_i^c, L_i, E_i^c)$ , with right-handed neutrino superfield,  $N_i^c$ , and the electroweak Higgs doublet superfields,  $(H_u, H_d)$ . The last term, relevant for the right-handed neutrino masses, contains a cutoff scale,  $M_*$ . The scalar component of the gauge singlet superfield  $S$  acts as an inflaton, and the  $B-L$  conjugate pair of Higgs superfields  $(\Phi, \bar{\Phi})$  provides the vacuum energy,  $\kappa^2 M^4$ , for inflation containing the  $B-L$  symmetry breaking scale  $M$ . The above superpotential not only possesses the local  $U(1)_{B-L}$  symmetry, but it also contains three global symmetries, namely,  $U(1)_R, U(1)_B$  and  $U(1)_L$ , with  $R(W) = 2$  and  $B(W) = 0 = L(W)$ . The charge assignments under these symmetries of the various matter and Higgs superfields are given in Table I.

The global SUSY minimum occurs at,

$$\langle S \rangle = 0, \quad \langle \Phi\bar{\Phi} \rangle = M^2, \quad \langle H_u \rangle = 0 = \langle H_d \rangle. \quad (2)$$

After the breaking of  $U(1)_{B-L}$  gauge symmetry, the last term in Eq. (1) gives rise to Majorana mass terms for the right-handed neutrinos,

$$M_{ij}^R = \lambda_{ij} \left( \frac{M}{M_*} \right) M. \quad (3)$$

With  $\lambda_{ij} \lesssim \mathcal{O}(1)$  and  $M_* \sim 10^{18}$  GeV, we obtain Majorana masses  $\lesssim 10^{14}$  GeV with the gauge symmetry breaking scale  $M \sim 10^{16}$  GeV. Therefore, the light neutrino masses are naturally generated via the seesaw mechanism. It is also

TABLE I. Global and local charges of superfields.

Superfields	R	B	L	$B-L$
$E_i^c$	1	0	-1	1
$N_i^c$	1	0	-1	1
$L_i$	1	0	1	-1
$U_i^c$	1	-1/3	0	-1/3
$D_i^c$	1	-1/3	0	-1/3
$Q_i$	1	1/3	0	1/3
$H_u$	0	0	0	0
$H_d$	0	0	0	0
$S$	2	0	0	0
$\Phi$	0	0	-1	1
$\bar{\Phi}$	0	0	1	-1

interesting to note that the  $R$ -parity which prevents rapid proton decay mediated by the dimension four operators appears as a  $Z_2$  subgroup of  $U(1)_R$  symmetry. However, the proton is essentially stable due to the global and local symmetries described in Table I. A  $Z_4$  subgroup of  $U(1)_R$  symmetry, consistent with the  $R$  charge assignment displayed in Table I, is identified as a unique anomaly free discrete symmetry described in [29] that forbids both the  $\mu$ -term and all dimension four and five baryon and lepton number violating operators in MSSM.

The superpotential term relevant for hybrid inflation is [1,2],

$$W = \kappa S(\Phi\bar{\Phi} - M^2), \quad (4)$$

and the global SUSY F-term scalar potential is given by,

$$V_F = \kappa^2 |M^2 - \phi\bar{\phi}|^2 + \kappa^2 |s|^2 (|\phi|^2 + |\bar{\phi}|^2), \quad (5)$$

where  $\phi, \bar{\phi}, s$  represents the bosonic components of the superfields  $\Phi, \bar{\Phi}, S$  respectively. In the D-flat direction,  $|\phi| = |\bar{\phi}|$ , using Eq. (4) and Eq. (5), we write the tree level global SUSY potential as,

$$V = V_0 [(1 - y^2)^2 + 2x^2 y^2], \quad (6)$$

where  $V_0 = \kappa^2 M^4$ ,  $x = |s|/M$  and  $y = |\phi|/M$ . This scalar potential is displayed in Fig. 1 where a flat direction ( $y = 0$ ) with  $x > 1$ , suitable for inflation, is clearly visible. As described below, the various important contributions to the scalar potential provide the necessary slope for the realization of inflation in the otherwise flat trajectory.

The F-term supergravity (SUGRA) scalar potential is given by,

$$V_F = e^{K/m_p^2} (K_{ij}^{-1} D_{z_i} W D_{z_j}^* W^* - 3m_p^{-2} |W|^2), \quad (7)$$

where,

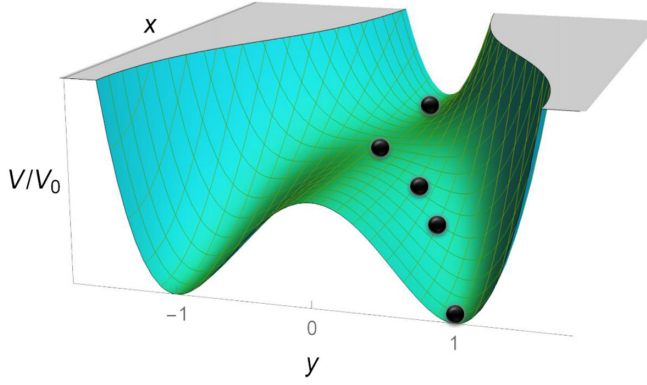


FIG. 1. The normalized global SUSY scalar potential  $V/V_0$  as a function of  $x = |s|/M$  and  $y = |\phi|/M$ .

$$D_{z_i} W \equiv \frac{\partial W}{\partial z_i} + m_P^{-2} \frac{\partial K}{\partial z_i} W, \quad K_{ij} \equiv \frac{\partial^2 K}{\partial z_i \partial z_j^*},$$

$D_{z_i^*} W^* = (D_{z_i} W)^*$ ,  $z_i \in \{\phi, \bar{\phi}, s\}$ , and  $m_P \simeq 2.4 \times 10^{18}$  GeV is the reduced Planck mass. In the present paper we employ the minimal (canonical) Kähler potential given by,

$$K = |S|^2 + |\Phi|^2 + |\bar{\Phi}|^2, \quad (8)$$

and the SUGRA corrections can now be calculated using the above definitions. Along the inflationary trajectory SUSY is broken due to the nonzero vacuum term,  $V_0$ . This generates a mass splitting between the fermionic and the bosonic components of the relevant superfields and leads to radiative corrections in the scalar potential [1]. Another important contribution in the scalar potential arises from the soft SUSY breaking terms [4,5,7].

Including the leading order SUGRA corrections, one-loop radiative corrections and the soft SUSY breaking terms, the scalar potential along the inflationary trajectory (i.e.,  $y = 0$ ) can be written as [7,12,14],

$$V \simeq V_0 \left[ 1 + \left(\frac{M}{m_P}\right)^4 \frac{x^4}{2} + \frac{\kappa^2}{8\pi^2} F(x) + \frac{\lambda^2}{4\pi^2} F(\sqrt{\gamma}x) + a \left(\frac{m_{3/2} x}{\kappa M}\right) + \left(\frac{M_S x}{\kappa M}\right)^2 \right], \quad (9)$$

where  $\gamma \equiv \lambda/\kappa$  and

$$F(x) = \frac{1}{4} \left[ (x^4 + 1) \ln \frac{(x^4 - 1)}{x^4} + 2x^2 \ln \frac{x^2 + 1}{x^2 - 1} + 2 \ln \frac{\kappa^2 M^2 x^2}{Q^2} - 3 \right], \quad (10)$$

is the one-loop radiative correction function evaluated at the renormalization scale  $Q$ , and  $a$  is defined as,

$$a = 2|2 - A| \cos[\arg s + \arg(2 - A)]. \quad (11)$$

The last two terms in Eq. (9) are the soft SUSY breaking linear and mass-squared terms, respectively, obtained in a gravity-mediated SUSY breaking scheme. The presence of  $a$ -term makes the present model a two-field inflation model [30]. However, we assume a suitable initial condition for  $\arg s$  so that  $a$  remains constant during inflation [12]. We further assume the soft mass,  $M_S$ , of the  $s$  field to be different, in general, from the gravitino mass,  $m_{3/2}$ . As we will see later, this choice provides an extra degree of freedom which yields a relatively wider range of  $M$  consistent with the central value of the spectral index  $n_s = 0.966$  measured by Planck 2018 [10]. The dimensionless parameter  $a$  and the soft mass squared,  $M_S^2$ , can have any sign. For standard SUSY hybrid inflation, it is shown in [7] that choosing the negative sign for either soft SUSY breaking term predicts the scalar spectral index  $n_s$  in good agreement with the central value reported by Planck 2018. We envisage similar results in the present  $\mu$ -hybrid inflation model.

### III. INFLATIONARY OBSERVABLES IN SLOW-ROLL APPROXIMATION

The prediction for the various inflationary parameters are estimated using the standard slow roll parameters defined as,

$$\epsilon = \frac{1}{4} \left(\frac{m_P}{M}\right)^2 \left(\frac{V'}{V}\right)^2, \quad \eta = \frac{1}{2} \left(\frac{m_P}{M}\right)^2 \left(\frac{V''}{V}\right),$$

$$\xi^2 = \frac{1}{4} \left(\frac{m_P}{M}\right)^4 \left(\frac{V'V'''}{V^2}\right), \quad (12)$$

where prime denotes the derivative with respect to  $x$ . Note that the extra factor of  $1/2$  is due to the relation between the canonically normalized real inflaton field,  $\sigma \equiv |s|/\sqrt{2}$ , and the complex field,  $s$ . In the slow-roll approximation, the scalar spectral index  $n_s$ , the tensor-to-scalar ratio  $r$  and the running of the scalar spectral index  $\alpha_s \equiv dn_s/d \ln k$  are given by,

$$n_s \simeq 1 + 2\eta - 6\epsilon, \quad r \simeq 16\epsilon,$$

$$\alpha_s \simeq 16\epsilon\eta - 24\epsilon^2 - 2\xi^2. \quad (13)$$

The value of the scalar spectral index  $n_s$  in the  $\Lambda$ CDM model is  $n_s = 0.9665 \pm 0.0038$  [9].

The amplitude of the scalar power spectrum is given by,

$$A_s(k_0) = \frac{1}{24\pi^2 \epsilon(x_0)} \left(\frac{V(x_0)}{m_P^4}\right), \quad (14)$$

where  $A_s(k_0) = 2.137 \times 10^{-9}$  at the pivot scale  $k_0 = 0.05 \text{ Mpc}^{-1}$  as measured by Planck 2018 [9]. The relevant number of  $e$ -folds,  $N_0$ , before the end of inflation is,

$$N_0 = 2 \left( \frac{M}{m_P} \right)^2 \int_{x_e}^{x_0} \left( \frac{V}{V'} \right) dx, \quad (15)$$

where  $x_0 \equiv x(k_0)$  is the field value at the pivot scale  $k_0$ , and  $x_e$  is the field value at the end of inflation. As the case may be, the value of  $x_e$  is fixed either by the breakdown of the slow roll approximation ( $\eta(x_e) = -1$ ), or by a ‘waterfall’ destabilization occurring at the value  $x_e = 1$ .

#### IV. REHEATING AND LEPTOGENESIS

After the end of inflation, the system falls toward the SUSY vacuum and performs damped oscillations about it. The inflaton consists of the two complex scalar fields  $s$  and  $\theta = (\delta\phi + \delta\bar{\phi})/\sqrt{2}$  with the same mass,  $m_{\text{inf}} \simeq \sqrt{2}\kappa M$ . The inflaton predominantly decays into a pair of Higgsinos ( $\tilde{h}_u, \tilde{h}_d$ ) and Higgses ( $h_u, h_d$ ), each with a decay width,  $\Gamma_h$ , given by [31],

$$\Gamma_h = \Gamma(\theta \rightarrow \tilde{h}_u \tilde{h}_d) = \Gamma(s \rightarrow h_u h_d) = \frac{\lambda^2}{8\pi} m_{\text{inf}}. \quad (16)$$

The other decay mode, via the superpotential couplings ( $\lambda_{ij}/M_* \bar{\Phi}^2 N_i^c N_j^c$ ), leads to a pair of right-handed neutrinos ( $N$ ) and sneutrinos ( $\tilde{N}$ ) respectively with equal decay width given as [32],

$$\begin{aligned} \Gamma_N &= \Gamma(\theta \rightarrow NN) = \Gamma(s \rightarrow \tilde{N}\tilde{N}) \\ &= \frac{m_{\text{inf}}}{8\pi} \left( \frac{M_N}{M} \right)^2 \left( 1 - \frac{4M_N^2}{m_{\text{inf}}^2} \right)^{1/2}, \end{aligned} \quad (17)$$

provided that only the lightest right-handed neutrino with mass  $M_N$  satisfies the kinematic bound,  $m_{\text{inf}} > 2M_N$ .

The relevant Boltzmann equations for the evolution of the total energy density,  $\rho$ , of  $s$  and  $\theta$  fields and the radiation energy density,  $\rho_r$ , are given by,

$$\dot{\rho} = -3H\rho - \Gamma_{\text{inf}}\rho, \quad \dot{\rho}_r = -4H\rho_r + \Gamma_{\text{inf}}\rho_r, \quad (18)$$

where,

$$H^2 = \frac{\rho + \rho_r}{3m_P^2} \quad \text{and} \quad \Gamma_{\text{inf}} = \Gamma_h + \Gamma_S. \quad (19)$$

With  $H = 3\Gamma_{\text{inf}}$ , we define the reheat temperature  $T_R$  in terms of the inflaton decay width  $\Gamma_{\text{inf}}$ ,

$$T_R = \left( \frac{90}{\pi^2 g_*} \right)^{1/4} \sqrt{\Gamma_{\text{inf}} m_P}, \quad (20)$$

where  $g_* = 228.75$  for MSSM. Note that the effect of preheating is expected to be suppressed in making the perturbative estimate for  $T_R$ . Assuming a standard thermal history, the number of  $e$ -folds,  $N_0$ , can be written in terms of the reheat temperature,  $T_R$ , as [33],

$$N_0 = 53 + \frac{1}{3} \ln \left[ \frac{T_R}{10^9 \text{ GeV}} \right] + \frac{2}{3} \ln \left[ \frac{\sqrt{\kappa} M}{10^{15} \text{ GeV}} \right]. \quad (21)$$

Note that the effect of preheating in supersymmetric hybrid inflation is generally expected to be suppressed [34,35]. However, if both the inflaton and waterfall fields are coupled to an additional scalar field, the preheating can be efficient if the inflaton is relatively strongly coupled to this scalar field [34]. In the present case, the electroweak Higgs doublet in the D-flat direction represents such a scalar field and efficient preheating requires  $\lambda \gg \kappa$ . As we only consider  $\lambda \sim \kappa$ , the non-perturbative effects via preheating are expected to be suppressed in our case. In addition, preheating associated with fermions is generically expected to be subdominant due to Pauli blocking.

Although subdominant,  $\Gamma_N/\Gamma_h \leq 1/(3\sqrt{3}\gamma^2) \simeq (0.4/\gamma)^2 < 1$ , the  $\Gamma_N$  channel is important for successful leptogenesis which is partially converted into the observed baryon asymmetry through the sphaleron process [36–38]. The washout factor of lepton asymmetry can be suppressed by assuming  $M_N \gg T_R$ . The observed baryon asymmetry is evaluated in term of the lepton asymmetry factor,  $\epsilon_L$ ,

$$\frac{n_B}{n_\gamma} \simeq -1.84\epsilon_L \frac{\Gamma_N}{\Gamma_{\text{inf}}} \frac{T_R}{m_{\text{inf}}} \delta_{\text{eff}}, \quad (22)$$

where  $\delta_{\text{eff}}$  is the  $CP$  violating phase factor,  $\Gamma_{\text{inf}} \simeq \Gamma_h$  and, assuming hierarchical neutrino masses,  $\epsilon_L$  is given by [39],

$$(-\epsilon_L) \simeq \frac{3}{8\pi} \frac{\sqrt{\Delta m_{31}^2} M_N}{\langle H_u \rangle^2}. \quad (23)$$

Here, the atmospheric neutrino mass squared difference is  $\Delta m_{31}^2 \approx 2.6 \times 10^{-3} \text{ eV}^2$  and  $\langle H_u \rangle \simeq 174 \text{ GeV}$  in the large  $\tan\beta$  limit. For the observed baryon-to-photon ratio,  $n_B/n_\gamma = (6.12 \pm 0.04) \times 10^{-10}$  [40], the bound on  $|\delta_{\text{eff}}| \leq 1$  along with the kinematic bound,  $m_{\text{inf}} \geq 2M_N$ , translates into a bound on the reheat temperature,

$$T_R \gtrsim \gamma^2 2 \times 10^7 \text{ GeV} \geq 2 \times 10^7 \text{ GeV}, \quad (24)$$

for  $\gamma \geq 1$ . In order to attain the minimum possible reheat temperature we set  $\gamma = 1$ . This bound from successful leptogenesis, i.e.  $T_R \gtrsim 2 \times 10^7 \text{ GeV}$ , is represented by the gray dashed line in Figs. 2–4. An underproduction of leptogenesis is assumed for  $T_R < 2 \times 10^7 \text{ GeV}$  with a reduction in  $M_N$ .

#### V. COSMIC STRING CONSTRAINTS

Cosmic strings (CSs) are produced at the end of inflation with implications related to anisotropies in the CMB and the production of stochastic gravitational waves (SGWs). The predictions related to SGWs are discussed in Sec. IX. The strength of the string’s gravitational interaction is



expressed in terms of the dimensionless string tension,  $G\mu_{cs}$ , where  $G = 1/8\pi m_p^2$  and  $\mu_{cs}$  is mass per unit length of the string. The CMB bound on the CS tension is [9,10],

$$G\mu_{cs} \lesssim 1.3 \times 10^{-7}. \quad (25)$$

The quantity  $\mu_{cs}$ , can be written in terms of the  $U(1)_{B-L}$  gauge symmetry breaking scale  $M$  [41],

$$\begin{aligned} \mu_{cs} &= 2\pi M^2 \epsilon(\beta), \\ \epsilon(\beta) &= \frac{2.4}{\log(2/\beta)} \quad \text{for } \beta = \frac{\kappa^2}{2g^2} < 10^{-2}, \end{aligned} \quad (26)$$

where  $g = 0.7$  for MSSM. Requiring  $M \lesssim 10^{16}$  GeV,  $G\mu_{cs} \lesssim 10^{-6}$  and this is possible with a metastable CS network as described in [23]. This possibility not only circumvents the CMB bound on  $G\mu_{cs}$ , it can also evade other bounds coming from LIGO O3 [42]. A possible realization of a metastable CS network in a GUT setup based on  $SO(10)$  model is described in Sec. IX.

### VI. RESULTS AND DISCUSSION

The seven parameters of the present model,  $\kappa, M, am_{3/2}, M_S^2, x_0, x_e,$  and  $M_N$ , are constrained by five conditions, namely, the amplitude of scalar power spectrum,  $A_s(k_0) = 2.137 \times 10^{-9}$  Eq. (14), the scalar spectral index,  $n_s = 0.9665$ , the end of inflation by the waterfall,  $x_e = 1$ , the number of  $e$ -folds,  $N_0$ , defined in Eq. (15) and given in terms of  $T_R$  by Eq. (21), and finally the observed value of baryon-to-photon ratio,  $n_B/n_\gamma = 6.12 \times 10^{-10}$  Eq. (22). This leaves two independent parameters to freely vary which can be taken to be  $am_{3/2}$  and  $M_S^2$ . Keeping one parameter fixed, the second can be varied as depicted in Figs. 2(a) and 2(b). In Fig. 2(a), we vary  $am_{3/2}$  for various values of  $M_S^2$  in the range  $2 \times 10^{12}$  GeV<sup>2</sup> to

$-2 \times 10^{17}$  GeV<sup>2</sup>. In Fig. 2(a), the curve with  $M_S \sim 0$  has already been discussed in [19] with a minimal (canonical) Kähler potential. On the other hand, the region with  $|M_S^2| \neq 0$  is the new parametric space explored in this paper. However, see [8] where this region is explored in the standard hybrid inflation model ( $\gamma \ll 1$ ). Similarly, in Fig. 2(b) we vary  $M_S^2$  for fixed values of  $m_{3/2}$  lying in the range from 0 to 730 TeV (0 to 155 GeV) for  $a = 1$  (-1).

In accordance with the outcome of SUSY hybrid inflation model [7,8], at least one of the two parameters,  $M_S^2$  or  $am_{3/2}$ , is expected to be negative in order to realize the red-tilted scalar spectral index consistent with Planck-2018 data. In the present model, the scalar spectral index with  $x_0 \sim 1$  can be written as,

$$n_s \simeq 1 + \left(\frac{m_P}{M}\right)^2 \left(2\left(\frac{M_S}{\kappa M}\right)^2 + 3\frac{\kappa^2}{8\pi^2} F''(x_0)\right). \quad (27)$$

In the limit where  $M_S^2$  term is dominant in the above expression we obtain,

$$\left(\frac{M_S}{\kappa M}\right)^2 \simeq -\frac{(1-n_s)}{2} \left(\frac{M}{m_P}\right)^2. \quad (28)$$

This explains the  $M \propto \kappa^{-1/2}$  behavior of the curves in Fig. 2(a) for most of the upper region with constant values of  $M_S^2$ . This behavior changes near the  $M_S \sim 0$  curve where the radiative term in Eq. (27) becomes dominant and thus predicting the  $M \propto \kappa$  behavior. Regarding the behavior of the corresponding curves in Fig. 2(b) with fixed values of  $am_{3/2} > 0$ , it is noted that the soft SUSY breaking terms compete with each other in  $\epsilon(x_0)$  in order to satisfy the constraint of  $A_s$  given in Eq. (14). Using this observation and Eq. (27) we obtain  $M \propto \kappa^{-1/3}$  which is consistent with the curves shown in the upper region of Fig. 2(b).

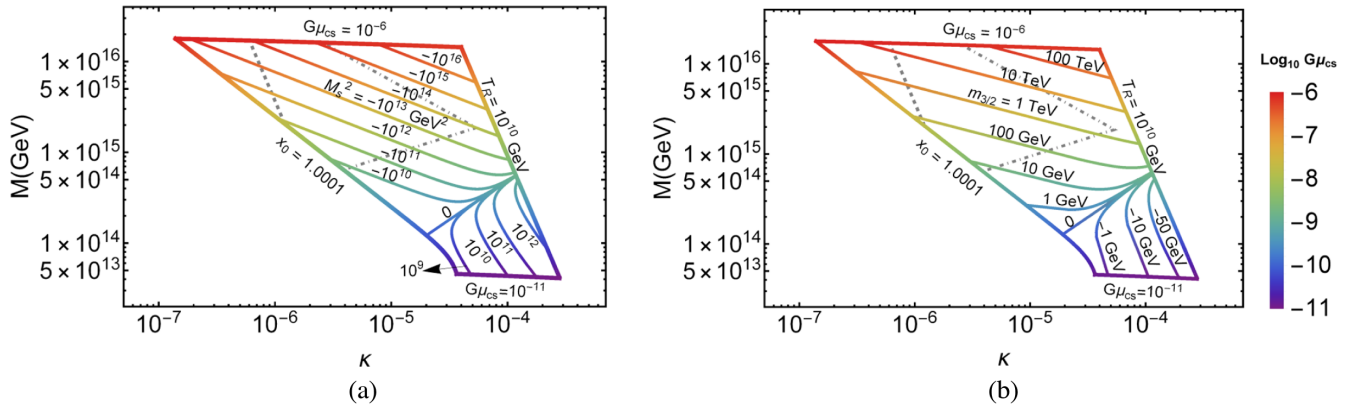


FIG. 2. The symmetry breaking scale  $M$  versus the coupling  $\kappa$ , with maximum (minimum) reheate temperature  $T_R$  of  $10^{10}$  GeV ( $2.3 \times 10^6$  GeV), and fine tuning bound of 0.01%. The rainbow color vertical bar represents the variation of the dimensionless string tension  $G\mu_{cs}$  from  $10^{-6}$  to  $10^{-11}$ . The inside mesh shows the variation of soft mass term  $M_S^2$  in (a), and that of gravitino mass  $m_{3/2}$ , in (b). Gray dashed line is the  $T_R$  bound of leptogenesis, and dot-dashed is of stable LSP gravitino DM.

For the case  $M_S^2 > 0$ , the radiative correction term starts to compete with the  $M_S^2$  term in Eq. (27) while moving away from the  $M_S \sim 0$  curve. This gives rise to  $M \propto \kappa^{-2}$  behavior as can be seen in the lower region of Fig. 2(a). Regarding the behavior of the corresponding region in Fig. 2(b) with fixed values of  $am_{3/2} > 0$ , it is noted that the soft SUSY breaking and radiative correction terms are comparable in  $\epsilon(x_0)$  in order to satisfy the constraint of  $A_s$  given in Eq. (14). This leads to  $M \propto \kappa^{-3}$  behavior of curves in the lower region of Fig. 2(b).

The four boundary curves in Figs. 2–4 are respectively described by  $G\mu_{cs} = 10^{-6}, 10^{-11}$ ,  $T_R = 10^{10}$  GeV and  $x_0 = 1.0001$ . We do not consider larger values of reheat temperature,  $T_R \gtrsim 10^{10}$  GeV, which are usually constrained by the gravitino overproduction problem and allow up to 0.01% difference between  $x_0$  and  $x_e = 1$ , since for smaller values of  $\kappa$  the corresponding field value  $x_0$  happens to lie closer to the waterfall point,  $x = 1$ .

Owing to its direct dependence on  $M$ , the various fixed values of  $G\mu$  are almost horizontal while having a weak dependence on  $\kappa$ . A wider range of the gauge symmetry breaking scale,  $10^{13} \lesssim M/\text{GeV} \lesssim 10^{16}$  is obtained, as compared to  $M_S \sim 0$  curve, where the range  $(1-6) \times 10^{15}$  GeV is realized. As shown in Fig. 3(a), the curves with fixed values of reheat temperature,  $T_R$ , ranging between  $2 \times 10^6$  GeV to  $10^{10}$  GeV follow  $M \propto \kappa^{-3}$  behavior obtained from eqs. (16) and (20). Further, the curves with fixed values of inflaton mass,  $m_{\text{inf}} \simeq \sqrt{2}\kappa M$ , ranging from  $2 \times 10^9$  GeV to  $8 \times 10^{11}$  GeV are shown in Fig. 3(b) and are consistent with  $M \propto \kappa^{-1}$  behavior.

The predicted range of the tensor to scalar ratio with tiny values,  $r \sim 5 \times 10^{-11} - 5 \times 10^{-21}$ , is shown in Fig. 4(a) where the various curves with constant values of  $r$  follow  $M \propto \kappa^{-1/2}$  behavior as can be obtained from Eq. (14),

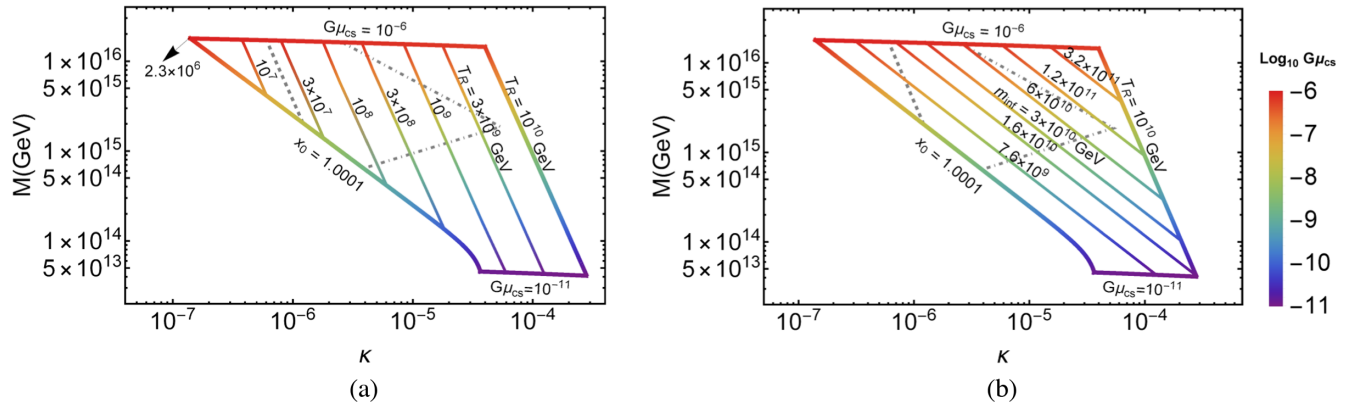


FIG. 3. The symmetry breaking scale  $M$  versus the coupling  $\kappa$ , with maximum (minimum) reheat temperature  $T_R$  of  $10^{10}$  GeV ( $2.3 \times 10^6$  GeV), and fine tuning bound of 0.01%. The rainbow color vertical bar represents the variation of the dimensionless string tension  $G\mu_{cs}$  from  $10^{-6}$  to  $10^{-11}$ . The inside mesh shows the variation of  $T_R$  in (a), and that of inflaton mass  $m_{\text{inf}}$  in (b). Gray dashed line is the  $T_R$  bound of leptogenesis, and dot-dashed is of stable LSP gravitino DM.

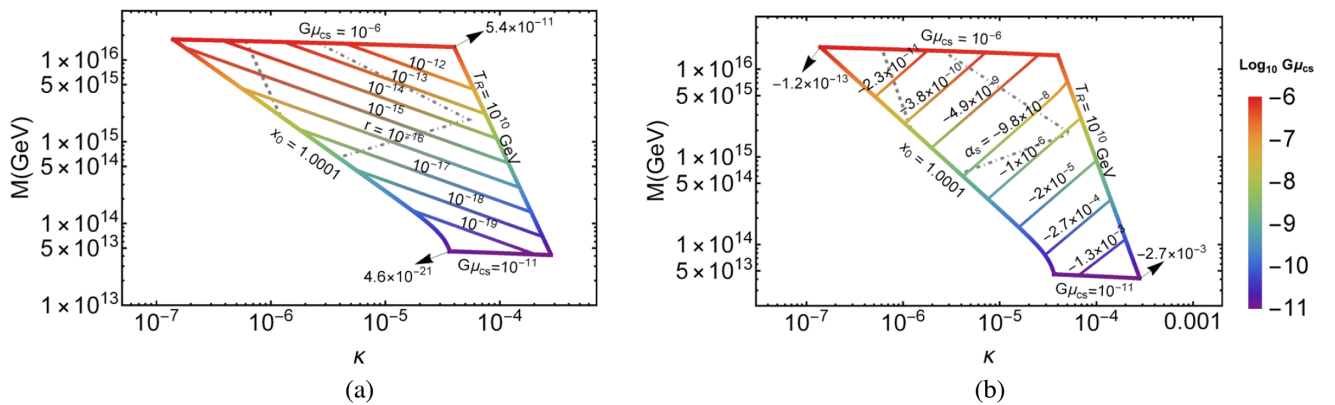


FIG. 4. The symmetry breaking scale  $M$  versus the coupling  $\kappa$ , with maximum (minimum) reheat temperature  $T_R$  of  $10^{10}$  GeV ( $2.3 \times 10^6$  GeV), and fine tuning bound of 0.01%. The rainbow color vertical bar represents the variation of the dimensionless string tension  $G\mu_{cs}$  from  $10^{-6}$  to  $10^{-11}$ . The inside mesh shows the variation of tensor to scalar ratio  $r$  in (a), and that of the running of spectral index  $\alpha_s$  in (b). Gray dashed line is the  $T_R$  bound of leptogenesis, and dot-dashed is of stable LSP gravitino DM.

$$r \sim \frac{2}{3\pi^2 A_s(k_0)} \frac{\kappa^2 M^4}{m_P^4}. \quad (29)$$

Finally, the relevant expression of  $\alpha_s$  in the slow-roll approximation is given by,

$$\alpha_s \simeq -\frac{1}{8} \left(\frac{m_P}{M}\right)^3 \left(12 \left(\frac{M}{m_P}\right)^4 x_0 + 3 \frac{\kappa^2}{8\pi^2} F'''(x_0)\right) \sqrt{r}. \quad (30)$$

The predicted range  $-\alpha_s \sim 2.7 \times 10^{-3} - 1.2 \times 10^{-13}$  is shown in Fig. 4(b) where the curves with constant values of  $\alpha_s$  follow  $M \propto \kappa$ , that can be obtained from Eq. (30) assuming a dominant contribution from the radiative correction with  $F'''(x_0) \propto \kappa^{-2}$ . The predicted ranges of  $r$  and  $\alpha_s$  with tiny values are consistent with the underlying assumption of the  $\Lambda$ CDM model.

### VII. GRAVITINO DARK MATTER

Following [17,19,20,43], an interesting realization of a stable gravitino as a cold dark matter (DM) candidate is presented here. The relic abundance for stable gravitinos is described in terms of the reheat temperature  $T_R$  and the gluino mass,  $m_{\tilde{g}}$ , as [44–47],

$$\Omega_{3/2} h^2 = 0.08 \left(\frac{T_R}{10^{10} \text{ GeV}}\right) \left(\frac{m_{3/2}}{1 \text{ TeV}}\right) \left(1 + \frac{m_{\tilde{g}}^2}{3m_{3/2}^2}\right). \quad (31)$$

This expression contains only the dominant QCD contributions for the gravitino production rate. The electroweak contribution [45] is expected to be relatively suppressed for our analysis. The observed DM abundance requires,  $\Omega_{3/2} h^2 \sim 0.12$  [9], which allows us to write the gravitino mass in terms of the reheat temperature for a given value of gluino mass. The gray dot-dashed curves in Figs. 2–4 are derived from Eq. (31) by taking into account  $m_{\tilde{g}} \gtrsim m_{3/2}$  and the LHC bound on the gluino mass,  $m_{\tilde{g}} > 2.2 \text{ TeV}$  [48]. The region to the left of these curves describes the gravitino DM in totality. It covers the values of gravitino mass in the range,  $m_{3/2} \sim 6 \text{ GeV} - 63 \text{ TeV}$  with reheat temperature up to  $6 \times 10^9 \text{ GeV}$ . Hence, the viable parameter space compatible with both DM and leptogenesis lies in the region bounded by the gray dashed and dot-dashed curves of Figs. 2–4. Assuming an underproduction of leptogenesis, the region left of the gray dot-dashed curve (see Figs. 2–4) is also compatible with gravitino DM.

With LSP gravitino the next to lightest supersymmetric particle (NLSP)  $\tilde{X}$  can decay into SM particles and gravitino. In this case the lifetime of  $\tilde{X}$  should be less than 1 sec in order to keep the successful predictions of big bang nucleosynthesis (BBN) intact. The decay rate for  $\tilde{X} \rightarrow \psi_\mu \gamma$  is given by [49],

$$\Gamma_{\tilde{X} \rightarrow \psi_\mu \gamma} \simeq \frac{\cos^2 \theta_W}{48\pi M_*^2} \frac{m_{\tilde{X}}^5}{m_{3/2}^2}, \quad (32)$$

where  $\theta_W$  is the electroweak mixing angle. For the NLSP lifetime,  $\tau_{\tilde{X}} \lesssim 1 \text{ sec}$ , Eq. (32) yields a lower bound on  $m_{3/2}$ ,

$$\left(\frac{m_{\tilde{X}}}{1 \text{ TeV}}\right) \text{ GeV} \lesssim m_{3/2} < m_{\tilde{X}}. \quad (33)$$

For  $m_{\tilde{X}} \sim 1 \text{ TeV}$  (10 TeV), we obtain  $1 \text{ GeV} \lesssim m_{3/2} < 1 \text{ TeV}$  ( $10 \text{ GeV} \lesssim m_{3/2} < 10 \text{ TeV}$ ). This again confirms that the region bounded by the gray dot-dashed and dashed curves is consistent with a gravitino DM and successful leptogenesis.

In order to suppress the washout effects in nonthermal leptogenesis we usually require  $M_N$  to be somewhat larger than  $T_R$ . This can be achieved in the present model by exploiting the freedom in the allowed range of the  $CP$ -violating phase factor,  $\delta_{\text{eff}} \leq 1$ . We can choose any value of the lightest right-handed neutrino mass,  $M_N$ , lying in the range,  $T_R \leq M_N \leq m_{\text{inf}}/2$ . For example with  $M_N = m_{\text{inf}}/4$  we obtain  $10 \lesssim M_N/T_R \lesssim 200$  consistent with gravitino DM scenario.

### VIII. UNSTABLE GRAVITINOS

We next consider the following two possibilities for unstable gravitinos:

- (1) Unstable long lived gravitino,  $m_{3/2} < 25 \text{ TeV}$ ,
- (2) Unstable short lived gravitino,  $m_{3/2} > 25 \text{ TeV}$ .

For the unstable long-lived gravitino,  $m_{3/2} < 25 \text{ TeV}$ , we have to take into account the BBN bounds on the reheat temperature [49,50],

$$2 \times 10^7 \text{ GeV} \lesssim T_R \lesssim 10^{10} \text{ GeV}, \quad (34)$$

which yields  $5 \text{ TeV} \lesssim m_{3/2} \lesssim 25 \text{ TeV}$ . For example, for a typical gravitino mass  $\sim 10 \text{ TeV}$ , the BBN bound on the reheat temperature,  $T_R \lesssim (1 - 2) \times 10^9 \text{ GeV}$ , is consistent with the predictions displayed in Figs. 2–4. Therefore, an unstable long-lived gravitino is viable for a wide range of reheat temperature described above.

For an unstable short lived gravitino,  $m_{3/2} > 25 \text{ TeV}$ , the BBN bounds on  $T_R$  are no more applicable. However, there is another constraint coming from the decay of gravitinos to the lightest sypersymmetric particle (LSP)  $\tilde{\chi}_1^0$ . In this case, the LSP relic density is given by, [49]

$$\Omega_{\tilde{\chi}_1^0} h^2 \simeq 2.8 \times 10^{10} \times Y_{3/2} \left(\frac{m_{\tilde{\chi}_1^0}}{100 \text{ GeV}}\right), \quad (35)$$

where  $m_{\tilde{\chi}_1^0}$  is the LSP mass, and  $Y_{3/2}$  is the gravitino yield given as,

$$Y_{3/2} \simeq 2.3 \times 10^{-18} \left( \frac{T_R}{10 \text{ TeV}} \right). \quad (36)$$

Requiring the LSP neutralino density to not exceed the DM relic density, Eq. (35) gives an upper bound on the neutralino mass,

$$m_{\tilde{\chi}_0^1} \lesssim 180 \left( \frac{10^{10} \text{ GeV}}{T_R} \right) \text{ GeV}, \quad (37)$$

which is consistent with the lower limit on the neutralino mass  $m_{\tilde{\chi}_0^1} \gtrsim 18 \text{ GeV}$  [51]. Using Eq. (37), the predicted range of  $T_R$  with successful leptogenesis (i.e.,  $10^{10} \text{ GeV} \gtrsim T_R \gtrsim 2 \times 10^7 \text{ GeV}$ ) can now be translated into a viable mass range for the LSP neutralino,

$$180 \text{ GeV} \lesssim m_{\tilde{\chi}_0^1} \lesssim 90 \text{ TeV}. \quad (38)$$

Thus, an unstable short-lived gravitino scenario is feasible for a wide range of LSP neutralino mass. This is in contrast to earlier studies of  $\mu$ -hybrid inflation with  $M_S \sim 0$  [19,20] where the feasibility of this scenario relies on a nonminimal Kähler potential.

## IX. GUT EMBEDDING AND METASTABLE COSMIC STRINGS

In a SUSY  $SO(10)$  framework, a metastable cosmic string network could arise via the symmetry breaking chain,

$$SO(10) \rightarrow \mathbb{G}_{\text{SM}} \times U(1)_\chi \rightarrow \mathbb{G}_{\text{SM}}, \quad (39)$$

where  $\mathbb{G}_{\text{SM}} \equiv SU(3)_c \times SU(2)_L \times U(1)_Y$  is the SM gauge group. The first breaking yields monopoles carrying SM and  $U(1)_\chi$  magnetic charges. The second breaking yields CSs with the string tension determined by the  $U(1)_\chi$  symmetry breaking scale [23,28]. Assuming that the monopoles are inflated away, the resulting string network is effectively metastable and yields a stochastic gravitational wave background spectrum that we explore in Sec. X. Note that the  $\chi$  charge coincides with  $B-L$  for  $Y = 0$ . For a recent discussion of metastable CS network formation in other gauge groups see [52]. The metastable string network decays via the Schwinger production of monopole-antimonopole pairs with a rate per string unit length of [23,53–55],

$$\Gamma_d = \frac{\mu_{\text{cs}}}{2\pi} \exp(-\pi\kappa_{\text{cs}}), \quad \kappa_{\text{cs}} = \frac{m^2}{\mu_{\text{cs}}}, \quad (40)$$

where  $m \sim M_G$  is the monopole mass and  $\kappa_{\text{cs}}$  quantifies the metastability of CSs network with  $\sqrt{\kappa_{\text{cs}}} \sim 10$  being the stability limit as the lifetime of CSs becomes larger than the age of the Universe. This parameter plays an important role

in making predictions for the current and future GW experimental tests.

## X. STOCHASTIC GRAVITATIONAL WAVE BACKGROUND FROM METASTABLE COSMIC STRINGS

The stochastic gravitational wave background (SGWB) emitted from the CS network is calculated in terms of the fractional energy density in GWs per logarithmic interval of frequency [56],

$$\Omega_{\text{GW}}(f) = \frac{8\pi G}{3H_0^2} f (G\mu_{\text{cs}})^2 \sum_{n=1}^{\infty} C_n(f) P_n. \quad (41)$$

Here,  $H_0 = 100h \text{ km/s/Mpc}$  is the Hubble parameter today with  $h = 0.68$  [10], and  $P_n$  is the power spectrum of GWs emitted by the  $n$ th harmonic of a CS loop. Our predictions are based on the Blanco-Pillado-Olum-Shlaer (BOS) model [56,57] and cusps as the main source of GWs with  $P_n$  given by [58],

$$P_n \simeq \frac{\Gamma}{\zeta\left[\frac{4}{3}\right]} n^{-4/3}, \quad (42)$$

where  $\Gamma \simeq 50$  is a numerical factor specifying the CSs decay rate and  $\zeta$  is the Riemann zeta function. It is convenient to work in terms of redshift  $z$  with  $1+z \equiv a_0/a(t)$  written in terms of the scale factor  $a(t)$  and its present value,  $a_0$ . The number of loops emitting GWs, observed at a given frequency  $f$  is defined as [56],

$$C_n(f) = \frac{2n}{f^2} \int_{z_{\text{min}}}^{z_{\text{max}}} \frac{dz}{H(z)(1+z)^6} \mathcal{N}(\ell, t). \quad (43)$$

The integration range corresponds to the life time of CSs network, from its formation at  $z_{\text{max}} \simeq \frac{T_R}{2.7K}^1$  until its decay at  $z_{\text{min}} = \left(\frac{70}{H_0}\right)^{1/2} \left(\frac{\Gamma(G\mu_{\text{cs}})^2}{2\pi \times 6.7 \times 10^{-39}} \exp(-\pi\kappa_{\text{cs}})\right)^{1/4}$  [59], and  $\mathcal{N}(\ell, t)$  is the number density of CS loop of length  $\ell = \frac{2n}{(1+z)f}$ .

The loop density is defined by considering their formation and decay in different epochs. In a radiation dominated era the loop density is given by [58],

$$\mathcal{N}_r(\ell, t) = \frac{0.18}{t^{2/3}(\ell + \Gamma G\mu_{\text{cs}} t)^{5/2}}, \quad (44)$$

with  $\ell \leq 0.1t$ , whereas in the matter era it is given by [58],

$$\mathcal{N}_m(\ell, t) = \frac{0.27 - 0.45(\ell/t)^{0.31}}{t^2(\ell + \Gamma G\mu_{\text{cs}} t)^2}, \quad (45)$$

<sup>1</sup> $T_R$  is taken to be around  $10^9 \text{ GeV}$ .



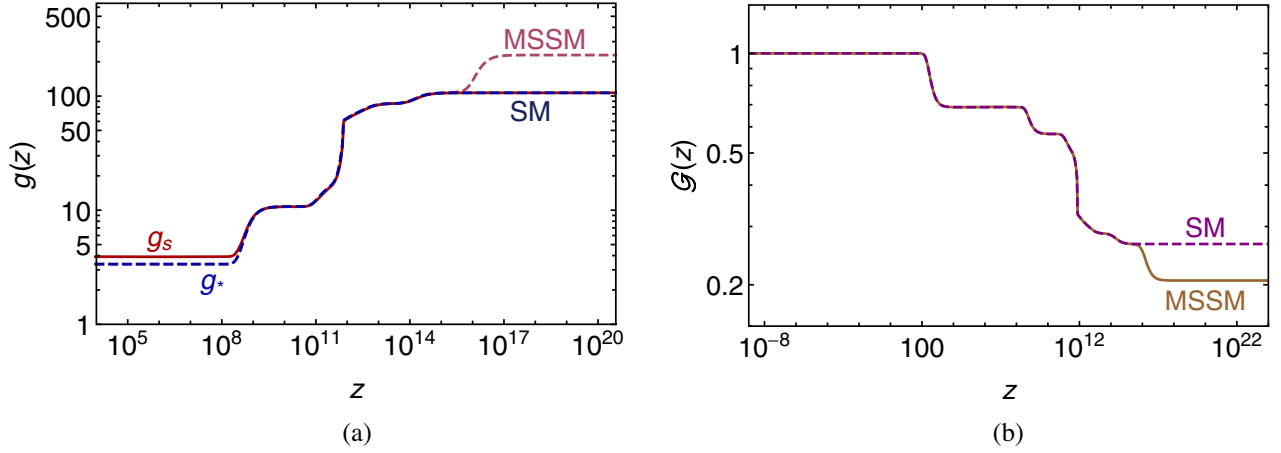


FIG. 5. (a) shows the evolution of effective degrees of freedom with redshift and (b) shows the evolution of  $\mathcal{G}$  as a function of redshift for both SM and MSSM.

with  $\ell < 0.18t$ . Lastly, the number density of loops produced during the radiation era, but radiating during the matter era is given by [58],

$$\mathcal{N}_{r,m}(\ell, t) = \frac{0.18(2H_0\sqrt{\Omega_{r,0}})^{3/2}}{(\ell + \Gamma G\mu_{cs}t)^{5/2}}(1+z)^3, \quad (46)$$

with  $\ell < 0.09t_{\text{eq}} - \Gamma G\mu_{cs}t$ .

The cosmological time as a function of  $z$  is written as [56],

$$t(z) = \int_z^{+\infty} \frac{dz'}{H(z')(1+z')}, \quad (47)$$

and the Hubble rate at redshift  $z$  is given by [56],

$$H(z) = H_0 \sqrt{\Omega_{\Lambda,0} + \Omega_{m,0}(1+z)^3 + \Omega_{r,0}\mathcal{G}(z)(1+z)^4}, \quad (48)$$

where  $\Omega_{m,0} = 0.31$ ,  $\Omega_{r,0} = \frac{4.15 \times 10^{-5}}{h^2}$  and  $\Omega_{\Lambda,0} = 1 - \Omega_{m,0}$  are the present values of matter, radiation and dark energy densities respectively, obtained from a standard flat  $\Lambda$ CDM model [10]. The function  $\mathcal{G}(z)$  defines the change in the expansion rate of the Universe due to annihilation of relativistic species at earlier times and is given as [60],

$$\mathcal{G}(z) = \frac{g_*(z)g_s^{4/3}(0)}{g_*(0)g_s^{4/3}(z)}, \quad (49)$$

where  $g_*(z)$ ,  $g_s(z)$  are the effective numbers of relativistic and entropic degrees of freedom respectively, at redshift  $z$ , and  $g_*(0)$ ,  $g_s(0)$  are their present values. The evolution of the effective degrees of freedom with redshift is shown in Figs. 5(a) and 5(b), both for the SM and MSSM.<sup>2</sup>

<sup>2</sup>We thanks Thomas Coleman for sharing the code.

Recently, NANOGrav has presented their 12.5-year data set [24] as a characteristic strain of the form,

$$h_{\text{strain}}(f) = A \left( \frac{f}{f_{\text{yr}}} \right)^{(3-\gamma_{cs})/2}, \quad (50)$$

where  $f_{\text{yr}} \equiv 1 \text{ yr}^{-1} = 32 \times 10^{-9} \text{ Hz}$ ,  $A$  is the strain amplitude and  $\gamma_{cs}$  is the slope or the spectral index which is related to the spectral GW energy density as,

$$\Omega_{\text{GW}}(f) = \frac{2\pi^2}{3H_0^2} f^2 h^2(f) = \Omega_{\text{yr}} \left( \frac{f}{f_{\text{yr}}} \right)^{5-\gamma_{cs}}, \quad (51)$$

with  $\Omega_{\text{yr}} \equiv \frac{2\pi^2 A^2 f_{\text{yr}}^2}{3H_0^2}$ . Taking the first two frequency bins of NANOGrav, i.e.,  $f_1 = 2.45 \times 10^{-9} \text{ Hz}$  and  $f_2 = 4.91 \times 10^{-9} \text{ Hz}$ , we obtain [61],

$$\gamma_{cs} = 5 - \frac{\ln(\Omega_{\text{GW}}(f_2)/\Omega_{\text{GW}}(f_1))}{\ln(2)} \quad \text{and} \quad A = \sqrt{\frac{3H_0^2 \Omega_{\text{GW}}(f_1) f_{\text{yr}}^{3-\gamma_{cs}}}{2\pi^2 f_1^{5-\gamma_{cs}}}}. \quad (52)$$

This leads to prediction for  $(\gamma_{cs}, A)$ , as shown in Fig. 6, with  $G\mu_{cs} = 10^{-6} - 10^{-11}$ ,  $\sqrt{\kappa_{cs}} \sim 7.5-9$ , and 10. Here the parameter  $\kappa_{cs}$  increases from left to right with  $\sqrt{\kappa_{cs}} = 10$  representing the stable CS limit and  $G\mu_{cs}$  decreases from top to bottom. The NANOGrav/PPTA [24,62]  $2\sigma$  ( $1\sigma$ ) posterior contours are shown by solid (dot-dashed) brown/orange region with a broken power law fit. The gray window in the upper right corner is the region excluded by the CMB constraint and is only applicable to CSs with lifetime longer than CMB decoupling, i.e.,  $\sqrt{\kappa_{cs}} \geq 8.6$ . The pink shaded region representing successful leptogenesis,

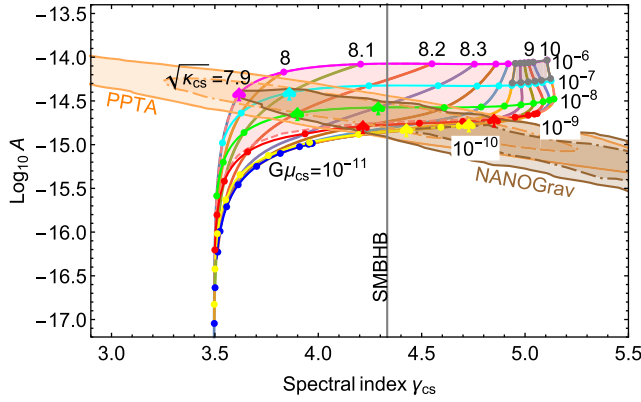


FIG. 6. The GWs signal from stable and metastable CSs compared to the NANOGrav observation for different values of  $G\mu_{\text{cs}}$  and  $\kappa_{\text{cs}}$ . Moving from top to bottom  $G\mu_{\text{cs}}$  varies between  $10^{-6}$  to  $10^{-11}$ , while moving from left to right  $\sqrt{\kappa_{\text{cs}}}$  varies between 7.5 to 9 and 10. The gray window in the upper right corner is the region excluded by CMB constraints, and the pink shaded region is for successful leptogenesis, DM and inflation. The brown/orange region, solid (dot-dashed), shows the  $2\sigma$  ( $1\sigma$ ) NANOGrav/PPTA posterior contours. The gray vertical line at  $\gamma_{\text{cs}} = 13/3$  represents the slope expected for supermassive black hole binary (SMBHB) mergers.

DM and inflation is congruous with the gray bounded region of Figs. 2–4.

In Fig. 7(a) the spectra of GW are shown for values of  $\sqrt{\kappa_{\text{cs}}}$  and  $G\mu_{\text{cs}}$  which lie within the  $2\sigma$  region of NANOGrav as indicated with corresponding color spades markers in Fig. 6. Ignoring dependence on the

effective degrees of freedom, the behavior  $\Omega_{\text{GW}} \propto f^{3/2}$  ( $\Omega_{\text{GW}} \propto f^0$ ) is achieved at the low (high) frequency range for the GW spectrum. This corresponds to the range  $\gamma_{\text{cs}} \sim 3.5$ –5 via Eq. (51) while explaining most of the predicted region shown in Fig. 6. The CS loops produced during the matter era and loops produced during the radiation era, but radiating during the matter era, become somewhat important in the low frequency range for  $\gamma_{\text{cs}} \gtrsim 5$ , but this region lies outside of the NANOGrav bounds. Due to pair production of GUT monopoles, the metastable long strings on superhorizon scales and string loops and segments on subhorizon scales cause a SGWB which we have not considered here but can be seen in [63].

For a detailed comparison of the various present (solid) and future (dashed) experiments, the allowed values of  $\sqrt{\kappa_{\text{cs}}}$  and  $G\mu_{\text{cs}}$  are shown in Fig. 7(b). It is interesting to note that metastable CS with  $\sqrt{\kappa_{\text{cs}}} \sim 8$ –9 allow  $G\mu_{\text{cs}} \sim 10^{-9}$ – $10^{-6}$ . Therefore, the gravitino DM scenario with successful leptogenesis in  $\mu$ -hybrid inflation, combined with NANOGrav SGWB, leads to the predicted range  $M_G \sim 10M \sim 10^{16}$  GeV– $10^{17}$  GeV for  $G\mu_{\text{cs}} \sim 10^{-9}$ – $10^{-6}$ . However, at larger frequencies, the range  $G\mu_{\text{cs}} \sim 10^{-8}$ – $10^{-6}$  is in some tension with the latest bounds from LIGO O3 [42]. But this tension still involves some theoretical and experimental uncertainties. A nonstandard thermal history [58,68–71], or late production of the CSs [72] can ameliorate this tension. Besides NANOGrav, we also show in Fig. 7(b) the observable region lying within the sensitivity bounds of future experiments, such as Einstein Telescope [66] and LISA [65].

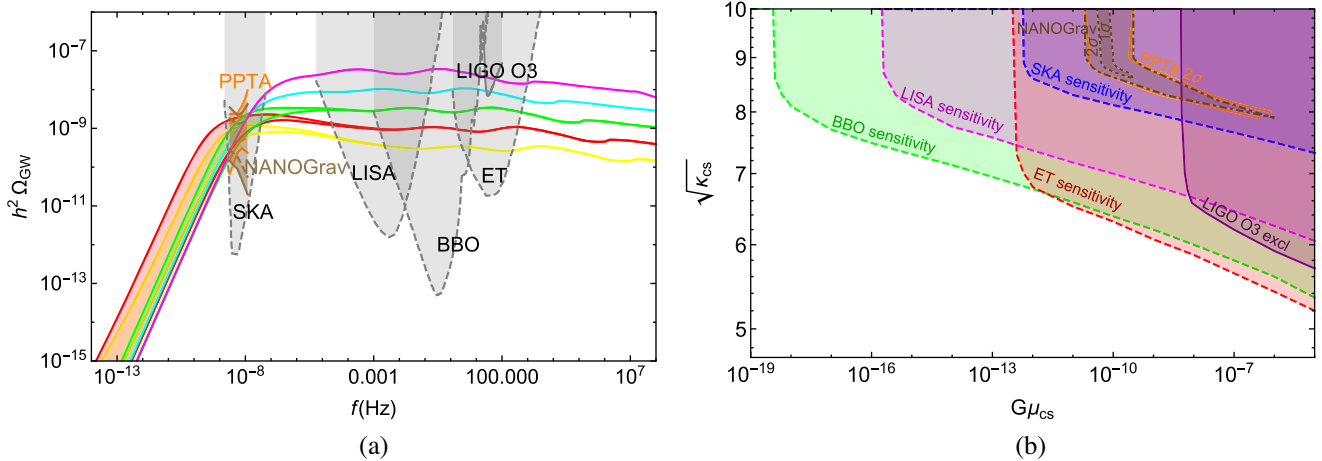


FIG. 7. (a) shows the GW spectra explaining the NANOGrav excess at  $2\sigma$  for allowed values of  $G\mu_{\text{cs}}$  with  $\sqrt{\kappa_{\text{cs}}} = 7.9$  to 9 and 10 as indicated with corresponding color spades markers in Fig. 6. The gray shaded regions indicate the sensitivity curves of present (solid boundaries) LIGO O3 [42] and future (dashed boundaries) SKA [64], LISA [65], ET [66], BBO [67] experiments. The brown/orange band solid (dashed) is the NANOGrav/PPTA  $2\sigma$  ( $1\sigma$ ). In (b), we display constraints on the CS parameter space from GW experiments. The solid lines are the regions excluded by existing bounds. The dashed line regions indicate the designed sensitivity of future experiments. The dot-dashed (small dashed) region is the NANOGrav excess at  $2\sigma$  and the orange region is PPTA  $2\sigma$ .

## XI. CONCLUSION

We have explored the  $\mu$ -hybrid inflation in a  $U(1)_{B-L}$  extension of the MSSM by considering both the linear and quadratic soft SUSY breaking terms with special focus on the parameter space described by  $|M_S| \gg m_{3/2}$ . A wide range of the gauge symmetry breaking scale,  $6 \times 10^{14} \lesssim M/\text{GeV} \lesssim 10^{16}$  is predicted for successful nonthermal leptogenesis and stable gravitino as a viable dark matter candidate. This parameter range corresponds to a stochastic gravitational wave background from a metastable cosmic string network with tension  $G\mu_{\text{cs}} \sim 10^{-9}-10^{-6}$ . Such a metastable cosmic string network can arise in a grand unified theory with  $U(1)_{B-L}$  embedded in an  $SO(10)$

model. An order of magnitude splitting is predicted between the GUT and  $B-L$  breaking scales. This connection certainly provides a unique opportunity to probe the seesaw mechanism and leptogenesis with gravitational waves [73–76]. The metastable cosmic string network lies within the  $2\sigma$  NANOGrav 12.5 year data/PPTA and is also within reach of future gravitational wave experiments.

## ACKNOWLEDGMENTS

This work is partially supported by the DOE Grant No. DE-SC0013880 (Q.S.). Adeela Afzal thanks Kai Schmitz, Valerie Domcke, Wilfried Buchmuller, Ken D. Olum and George Lazarides for useful discussion.

- 
- [1] G. R. Dvali, Q. Shafi, and Robert K. Schaefer, Large Scale Structure and Supersymmetric Inflation without Fine Tuning, *Phys. Rev. Lett.* **73**, 1886 (1994).
  - [2] Edmund J. Copeland, Andrew R. Liddle, David H. Lyth, Ewan D. Stewart, and David Wands, False vacuum inflation with Einstein gravity, *Phys. Rev. D* **49**, 6410 (1994).
  - [3] Andrei D. Linde and Antonio Riotto, Hybrid inflation in supergravity, *Phys. Rev. D* **56**, R1841 (1997).
  - [4] Vedat Nefer Senoguz and Q. Shafi, Reheat temperature in supersymmetric hybrid inflation models, *Phys. Rev. D* **71**, 043514 (2005).
  - [5] Wilfried Buchmuller, Laura Covi, and David Delepine, Inflation and supersymmetry breaking, *Phys. Lett. B* **491**, 183 (2000).
  - [6] Vedat Nefer Senoguz and Q. Shafi, Testing supersymmetric grand unified models of inflation, *Phys. Lett. B* **567**, 79 (2003).
  - [7] Mansoor Ur Rehman, Qaisar Shafi, and Joshua R. Wickman, Supersymmetric hybrid inflation redux, *Phys. Lett. B* **683**, 191 (2010).
  - [8] Mansoor Ur Rehman, Qaisar Shafi, and Joshua R. Wickman, Minimal supersymmetric hybrid inflation, flipped SU(5) and proton decay, *Phys. Lett. B* **688**, 75 (2010).
  - [9] Y. Akrami *et al.*, Planck 2018 results. X. Constraints on inflation, *Astron. Astrophys.* **641**, A10 (2020).
  - [10] N. Aghanim *et al.*, Planck 2018 results. VI. Cosmological parameters, *Astron. Astrophys.* **641**, A6 (2020).
  - [11] M. Bastero-Gil, S. F. King, and Q. Shafi, Supersymmetric hybrid inflation with non-minimal Kahler potential, *Phys. Lett. B* **651**, 345 (2007).
  - [12] Mansoor ur Rehman, Vedat Nefer Senoguz, and Qaisar Shafi, Supersymmetric and smooth hybrid inflation in the light Of WMAP3, *Phys. Rev. D* **75**, 043522 (2007).
  - [13] Qaisar Shafi and Joshua R. Wickman, Observable gravity waves from supersymmetric hybrid inflation, *Phys. Lett. B* **696**, 438 (2011).
  - [14] Mansoor Ur Rehman, Qaisar Shafi, and Joshua R. Wickman, Observable gravity waves from supersymmetric hybrid inflation II, *Phys. Rev. D* **83**, 067304 (2011).
  - [15] Waqas Ahmed, Athanasios Karozas, George K. Leontaris, and Umer Zubair, Smooth hybrid inflation with low reheat temperature and observable gravity waves in  $SU(5) \times U(1)_\gamma$  super-GUT, [arXiv:2201.12789](https://arxiv.org/abs/2201.12789).
  - [16] G. R. Dvali, George Lazarides, and Q. Shafi, Mu problem and hybrid inflation in supersymmetric SU(2)-L  $\times$  SU(2)-R  $\times$  U(1)-(B-L), *Phys. Lett. B* **424**, 259 (1998).
  - [17] Nobuchika Okada and Qaisar Shafi,  $\mu$ -term hybrid inflation and split supersymmetry, *Phys. Lett. B* **775**, 348 (2017).
  - [18] S. F. King and Q. Shafi, Minimal supersymmetric SU(4)  $\times$  SU(2)-L  $\times$  SU(2)-R, *Phys. Lett. B* **422**, 135 (1998).
  - [19] Mansoor Ur Rehman, Qaisar Shafi, and Fariha K. Vardag,  $\mu$ -hybrid inflation with low reheat temperature and observable gravity waves, *Phys. Rev. D* **96**, 063527 (2017).
  - [20] George Lazarides, Mansoor Ur Rehman, Qaisar Shafi, and Fariha K. Vardag, Shifted  $\mu$ -hybrid inflation, gravitino dark matter, and observable gravity waves, *Phys. Rev. D* **103**, 035033 (2021).
  - [21] John Ellis, Jihn E. Kim, and D. V. Nanopoulos, Cosmological gravitino regeneration and decay, *Phys. Lett. B* **145B**, 181 (1984).
  - [22] M. Yu. Khlopov and Andrei D. Linde, Is it easy to save the gravitino?, *Phys. Lett.* **138B**, 265 (1984).
  - [23] Wilfried Buchmuller, Valerie Domcke, Hitoshi Murayama, and Kai Schmitz, Probing the scale of grand unification with gravitational waves, *Phys. Lett. B* **809**, 135764 (2020).
  - [24] Zaven Arzoumanian *et al.*, The NANOGrav 12.5 yr data set: Search for an isotropic stochastic gravitational-wave background, *Astrophys. J. Lett.* **905**, L34 (2020).
  - [25] Waqas Ahmed, M. Junaid, Salah Nasri, and Umer Zubair, Constraining the cosmic strings gravitational wave spectra in no scale inflation with viable gravitino dark matter and non thermal leptogenesis, [arXiv:2202.06216](https://arxiv.org/abs/2202.06216).

- [26] Vedat Nefer Senoguz and Q. Shafi, U(1)(B-L): Neutrino physics and inflation, [arXiv:hep-ph/0512170](https://arxiv.org/abs/hep-ph/0512170).
- [27] C. Pallis, Gravitational waves,  $\mu$  term and leptogenesis from  $B-L$  Higgs inflation in supergravity, *Universe* **4**, 13 (2018).
- [28] Muhammad Atif Masoud, Mansoor Ur Rehman, and Qaisar Shafi, Sneutrino tribrid inflation, metastable cosmic strings and gravitational waves, *J. Cosmol. Astropart. Phys.* **11** (2021) 022.
- [29] Hyun Min Lee, Stuart Raby, Michael Ratz, Graham G. Ross, Roland Schieren, Kai Schmidt-Hoberg, and Patrick K. S. Vaudrevange, A unique  $\mathbb{Z}_4^R$  symmetry for the MSSM, *Phys. Lett. B* **694**, 491 (2011).
- [30] Wilfried Buchmüller, Valerie Domcke, Kohei Kamada, and Kai Schmitz, Hybrid inflation in the complex plane, *J. Cosmol. Astropart. Phys.* **07** (2014) 054.
- [31] George Lazarides and N. D. Vlachos, Atmospheric neutrino anomaly and supersymmetric inflation, *Phys. Lett. B* **441**, 46 (1998).
- [32] T. Asaka, Koichi Hamaguchi, M. Kawasaki, and T. Yanagida, Leptogenesis in inflationary universe, *Phys. Rev. D* **61**, 083512 (2000).
- [33] Andrew R. Liddle and Samuel M. Leach, How long before the end of inflation were observable perturbations produced?, *Phys. Rev. D* **68**, 103503 (2003).
- [34] Juan Garcia-Bellido and Andrei D. Linde, Preheating in hybrid inflation, *Phys. Rev. D* **57**, 6075 (1998).
- [35] M. Bastero-Gil, S. F. King, and J. Sanderson, Preheating in supersymmetric hybrid inflation, *Phys. Rev. D* **60**, 103517 (1999).
- [36] V. A. Kuzmin, V. A. Rubakov, and M. E. Shaposhnikov, On the anomalous electroweak baryon number nonconservation in the early universe, *Phys. Lett.* **155B**, 36 (1985).
- [37] M. Fukugita and T. Yanagida, Baryogenesis without grand unification, *Phys. Lett. B* **174**, 45 (1986).
- [38] S. Yu. Khlebnikov and M. E. Shaposhnikov, The statistical theory of anomalous fermion number nonconservation, *Nucl. Phys.* **B308**, 885 (1988).
- [39] Mansoor Ur Rehman, Mian Muhammad Azeem Abid, and Amna Ejaz, New inflation in supersymmetric SU(5) and flipped SU(5) GUT models, *J. Cosmol. Astropart. Phys.* **11** (2020) 019.
- [40] P. A. Zyla *et al.*, Review of particle physics, *Prog. Theor. Exp. Phys.* **2020**, 083C01 (2020).
- [41] Christopher T. Hill, Hardy M. Hodges, and Michael S. Turner, Variational Study of Ordinary and Superconducting Cosmic Strings, *Phys. Rev. Lett.* **59**, 2493 (1987).
- [42] R. Abbott *et al.*, Upper limits on the isotropic gravitational-wave background from Advanced LIGO and Advanced Virgo's third observing run, *Phys. Rev. D* **104**, 022004 (2021).
- [43] Waqas Ahmed, Athanasios Karozas, and George K. Leontaris, Gravitino dark matter, nonthermal leptogenesis, and low reheating temperature in no-scale Higgs inflation, *Phys. Rev. D* **104**, 055025 (2021).
- [44] M. Bolz, A. Brandenburg, and W. Buchmüller, Erratum to: Thermal production of gravitinos [*Nucl. Phys.* **B606**, 518 (2001)], *Nucl. Phys.* **B790**, 336 (2008).
- [45] Josef Pradler and Frank Daniel Steffen, Thermal gravitino production and collider tests of leptogenesis, *Phys. Rev. D* **75**, 023509 (2007).
- [46] Andrea Addazi and Maxim Yu. Khlopov, Dark matter from Starobinsky supergravity, *Mod. Phys. Lett. A* **32**, 1740002 (2017).
- [47] Helmut Eberl, Ioannis D. Gialamas, and Vassilis C. Spanos, Gravitino thermal production revisited, *Phys. Rev. D* **103**, 075025 (2021).
- [48] Tamas Almos Vami, Searches for gluinos and squarks, *Proc. Sci., LHCP2019* (2019) 168.
- [49] Masahiro Kawasaki, Kazunori Kohri, Takeo Moroi, and Akira Yotsuyanagi, Big-bang nucleosynthesis and gravitino, *Phys. Rev. D* **78**, 065011 (2008).
- [50] Masahiro Kawasaki, Kazunori Kohri, Takeo Moroi, and Yoshitaro Takaesu, Revisiting big-bang nucleosynthesis constraints on long-lived decaying particles, *Phys. Rev. D* **97**, 023502 (2018).
- [51] Dan Hooper and Tilman Plehn, Supersymmetric dark matter: How light can the LSP be?, *Phys. Lett. B* **562**, 18 (2003).
- [52] Wilfried Buchmuller, Metastable strings and dumbbells in supersymmetric hybrid inflation, *J. High Energy Phys.* **04** (2021) 168.
- [53] Louis Leblond, Benjamin Shlaer, and Xavier Siemens, Gravitational waves from broken cosmic strings: The bursts and the beads, *Phys. Rev. D* **79**, 123519 (2009).
- [54] A. Monin and M. B. Voloshin, The spontaneous breaking of a metastable string, *Phys. Rev. D* **78**, 065048 (2008).
- [55] A. Monin and M. B. Voloshin, Destruction of a metastable string by particle collisions, *Phys. At. Nucl.* **73**, 703 (2010).
- [56] Jose J. Blanco-Pillado and Ken D. Olum, Stochastic gravitational wave background from smoothed cosmic string loops, *Phys. Rev. D* **96**, 104046 (2017).
- [57] Jose J. Blanco-Pillado, Ken D. Olum, and Benjamin Shlaer, The number of cosmic string loops, *Phys. Rev. D* **89**, 023512 (2014).
- [58] Pierre Auclair *et al.*, Probing the gravitational wave background from cosmic strings with LISA, *J. Cosmol. Astropart. Phys.* **04** (2020) 034.
- [59] Wilfried Buchmuller, Valerie Domcke, and Kai Schmitz, From NANOGrav to LIGO with metastable cosmic strings, *Phys. Lett. B* **811**, 135914 (2020).
- [60] Pierre Binetruy, Alejandro Bohe, Chiara Caprini, and Jean-Francois Dufaux, Cosmological backgrounds of gravitational waves and eLISA/NGO: Phase transitions, cosmic strings and other sources, *J. Cosmol. Astropart. Phys.* **06** (2012) 027.
- [61] Jose J. Blanco-Pillado, Ken D. Olum, and Jeremy M. Wachter, Comparison of cosmic string and superstring models to NANOGrav 12.5-year results, *Phys. Rev. D* **103**, 103512 (2021).
- [62] Boris Goncharov *et al.*, On the evidence for a common-spectrum process in the search for the nanohertz gravitational-wave background with the Parkes Pulsar Timing Array, *Astrophys. J. Lett.* **917**, L19 (2021).
- [63] Wilfried Buchmuller, Valerie Domcke, and Kai Schmitz, Stochastic gravitational-wave background from metastable cosmic strings, *J. Cosmol. Astropart. Phys.* **12** (2021) 006.
- [64] R. Smits, M. Kramer, B. Stappers, D. R. Lorimer, J. Cordes, and A. Faulkner, Pulsar searches and timing with the square kilometre array, *Astron. Astrophys.* **493**, 1161 (2009).
- [65] Pau Amaro-Seoane *et al.*, Laser interferometer space antenna, [arXiv:1702.00786](https://arxiv.org/abs/1702.00786).



- [66] M. Punturo *et al.*, The Einstein Telescope: A third-generation gravitational wave observatory, *Classical Quantum Gravity* **27**, 194002 (2010).
- [67] Vincent Corbin and Neil J. Cornish, Detecting the cosmic gravitational wave background with the big bang observer, *Classical Quantum Gravity* **23**, 2435 (2006).
- [68] Chia-Feng Chang and Yanou Cui, Gravitational waves from global cosmic strings and cosmic archaeology, *J. High Energy Phys.* 03 (2022) 114.
- [69] Yanou Cui, Marek Lewicki, David E. Morrissey, and James D. Wells, Cosmic archaeology with gravitational waves from cosmic strings, *Phys. Rev. D* **97**, 123505 (2018).
- [70] Yann Gouttenoire, Géraldine Servant, and Peera Simakachorn, Beyond the standard models with cosmic strings, *J. Cosmol. Astropart. Phys.* 07 (2020) 032.
- [71] Yann Gouttenoire, Geraldine Servant, and Peera Simakachorn, Kination cosmology from scalar fields and gravitational-wave signatures, [arXiv:2111.01150](https://arxiv.org/abs/2111.01150).
- [72] George Lazarides, Rinku Maji, and Qaisar Shafi, Cosmic strings, inflation, and gravity waves, *Phys. Rev. D* **104**, 095004 (2021).
- [73] Jeff A. Dror, Takashi Hiramatsu, Kazunori Kohri, Hitoshi Murayama, and Graham White, Testing the Seesaw Mechanism and Leptogenesis with Gravitational Waves, *Phys. Rev. Lett.* **124**, 041804 (2020).
- [74] Simone Blasi, Vedran Brdar, and Kai Schmitz, Fingerprint of low-scale leptogenesis in the primordial gravitational-wave spectrum, *Phys. Rev. Research* **2**, 043321 (2020).
- [75] Rome Samanta and Satyabrata Datta, Gravitational wave complementarity and impact of NANOGrav data on gravitational leptogenesis, *J. High Energy Phys.* 05 (2021) 211.
- [76] Rome Samanta and Satyabrata Datta, Probing leptogenesis and pre-BBN universe with gravitational waves spectral shapes, *J. High Energy Phys.* 11 (2021) 017.